Theor Chim Acta (1987) 71: 59-73

Theoretica Chimica Acta

The role of the π-bonding network for trigonal level splittings of tris-bidentate $Cr(acac)_3$ and $Cr(ox)_3^{3-}$

M. A. Atanasov*, T. Schönherr and H.-H. Schmidtke

Institut für Theoretische Chemie der Universität Düsseldorf, Universitätsstrasse 1, D-4000 Düsseldorf 1, Federal Republic of Germany

(Received September 24, revised and accepted December 5, 1986)

The varying π-bonding contributions in the title compounds caused by the different electronic and molecular structure of the chelate rings are used for explaining the large band splittings in the absorption spectra by trigonal symmetry. It is shown that usual ligand field theory and the angular overlap model are not able to account for the trigonal level splitting of $Cr(acac)_3$ for which the coordination sphere of oxygen atoms is nearly octahedrally arranged. The experimental finding can, however, be rationalized by an extended angular overlap model which considers the phase coupling of π-orbitals in the ligands leading to non-additive contributions to the metal-ligand bond energy.

Key words: Angular overlap model — Orbital phase coupling — π-Bonding

1. Introduction

The angular overlap model (AOM) since its first application to rare earth complex compounds [1] has become a useful tool for treating molecular and electronic structures of a variety of compounds [2-4]. In particular for rationalizing the electronic level scheme of transition group compounds this model has turned out to be more generally applicable than common ligand field theory (LFT). Since the AOM can be easily extended using the guidelines given by MO-LCAO theory, the model is able to consider (possibly different) π-interactions and the

* On leave of absence from the Bulgarian Academy of Sciences, Sofia, Bulgaria

non-additivity of metal-ligand interactions more appropriately [5–7]. The problem which of the extensions have to be used and in what occasions is by no means trivial and must be considered more closely in the future.

The present work tries to contribute to this solution by looking at a relatively simple case, i.e., of tris-bidentate compounds with ligands containing a π-conjugated system which for a donor ligand interferes with metal d-orbitals by their highest occupied orbitals (HOMO). One of its representative, viz. $Cr(acac)_3$, acac = acetylacetonate, namely shows an electronic spectrum with a polarized band pattern [8] indicating large trigonal level splittings although the oxygen atoms coordinated to the central ion have according to the X-ray analysis an almost exact octahedral conformation [9]. This is unusual, since other metal-oxygen chromophores of bidentate ligands, e.g. $Cr(ox)_3^{3-}$, ox = oxalate, exhibiting equally large band splittings and polarization effects [10] have nuclear frameworks which are distorted to trigonal symmetry to a rather large extent [11]. The spectrum of $Cr(acac)_3$ not expected from the symmetry of the compound nor from a Jahn–Teller effect in the excited state (vide infra) must be explained by a change in the electronic structure due to π-bonding interaction which is not properly accounted for by either LFT nor by the common AOM. Although a LFT treatment is able to calculate an energy level scheme which rationalizes the band splittings in the $Cr(acac)_3$ spectrum, the parameters obtained from the fitting procedure are, however, in variance with any physical meaning concerning reasonable radial parts of d-electron wave functions [12]. Also the ligand field parameters extracted from experiment cannot be used for determining the trigonal distortions as carried out for other complex compounds where data are obtained in agreement with X-ray results [13, 14]. In a case study we will apply the AOM and its different extensions to the level schemes of $Cr(acac)_3$ and $Cr(ox)_3^{3-}$ showing which of these models is suitable for explaining spectral band polarisations and trigonal band splittings for a given molecular structure demonstrating also why a particular model works in one case and not in the other. Due to the large experimental body which is available for chromium(III) compounds in particular for tris-bidentate complexes the title compounds doped in their aluminium host lattices are chosen for comparison. Since there are some inconsistencies in the literature concerning experimental results, the low temperature polarized spectra of these compounds are reported in addition yielding some more details in the band features which are important for the present interpretation.

2. Theory

2.1. Geometry considerations

Geometric distortions of $M(A-A)_3$ chelates where $A-A$ is a bidentate ligand are best described by using a trigonal arrangement with respect to cartesian coordinates (cf. Fig. 1). The geometry of the MA_6 chromophore with equal metal ligand distances (symmetry D_3) is given by the polar angle θ and the twist angle ϕ assuming at angles $\phi = 0°$ and $\phi = 60°$ the higher symmetry arrangements of a trigonal prism (D_{3h}) and trigonal antiprism (D_{3d}), respectively. The distortion

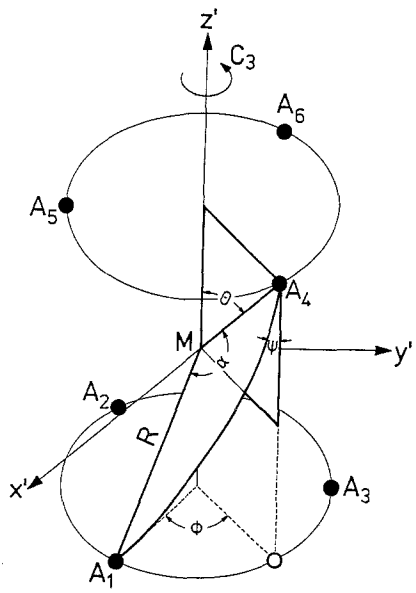

Fig. 1. Structural angles for symmetrically coordinated tris-bidentate complexes

is defined as a deviation from octahedral symmetry O_h at angles $\theta_{O_h} = 54.74°$ and $\phi_{O_h} = 60°$. For convenience we consider in addition the bite angle $\alpha = \sphericalangle AMA$ which describes the way the bidentate ligand is coordinated to the central ion and a diheder angle ψ defined by the angle between the *AMA* ligand plane and the plane containing the trigonal axis C_3 and the $M-A$ bond vector (cf. Fig. 1). For planar chelate ligands these angles are not independent, their relations

$$\cos\psi = \cos\theta \cdot \cos(\phi/2)/\sin(\alpha/2) \tag{1}$$

$$\cos(\alpha/2) = \sin\theta \cdot \cos(\phi/2) \tag{2}$$

which are briefly derived in Appendix 1, are more convenient than those given in the literature [6, 15] being in part also in error [15].

In the oxalate compound the ligands are not planar anymore, the molecules being twisted by an angle of $\gamma = 6°$–$7°$ around the $C-C$ axes. In this case an angle ψ at atoms A is defined which is equal on both ends of the chelate *AMA*, however, the equation (1) does not hold anymore, since ψ now varies freely not depending on θ and ϕ. Acetylacetonate ligands on the other hand retain their planar structure on complexation so that for these compounds the relations Eq. (1) and (2) must be fulfilled. The actual geometry parameters for the molecules considered as well as their iso-structural host compounds are calculated from the atomic coordinates obtained from X-ray investigations [9, 11, 16]; they are listed in Table 1. A comparison with octahedral values shows no significant deviation for the acetylacetonate complexes, however, for the oxalate compounds appreciable distortion particular for the angles α, ϕ and ψ is noticed.

2.2. Angular overlap models

For an outline of the concepts used in conventional AOM (model *a–c* in the flow diagram Table 2) it is referred to the literature [1–3, 15]. A presentation of

Table 1. Geometry parameters for chromium(III) and aluminium(III) acetylacetonate and oxalate complexes

Parameter	R (Å)[a]	α(°)	θ(°)	ϕ(°)	ψ(°)	γ(°)
O_h		90	54.74	60	45	—
$Cr(acac)_3$[b]	1.955	91.1	54.6	61.5	45.7	0
$Al(acac)_3$[c]	1.892	91.8	53.8	60.8	44.8	0
$K_3[Cr(ox)_3]\cdot 3H_2O$[d]	1.969	82.3	55.5	47.9	40.3	6.9
$K_3[Al(ox)_3]\cdot 3H_2O$[d]	1.896	83.7	54.4	47.3	38.9	5.9

[a] mean value, the actual interatomic distances differing in the last significant figure
[b] [9]
[c] [16]
[d] [11]

its formalism is not necessary here. One possible extension of this model distinguishes between different π-contributions $e_{\pi s}$ and $e_{\pi c}$ to the metal-ligand bond abandoning the "isotropic" electron distribution of linear symmetry around this axis (model d). This assumption is suggested, e.g., for chelate ligands where different π-bonding in plane and out of plane can be defined. Evidently the model should then put up different parameters $e_{\pi c} \equiv e_{\pi\parallel}$ and $e_{\pi s} \equiv e_{\pi\perp}$ for the metal-ligand π interaction by the use of, respectively, in plane and out of plane ligand orbitals [17]. A closer inspection of this model shows, however, that in the case of an octahedral arrangement where the structural angle takes the value $\psi = 45°$, always a "pseudoisotropic" electron density results, also when different parameter values $e_{\pi s}$ and $e_{\pi c}$ are chosen (model e). This is due to the trigonally quantized d-orbital basis chosen on grounds of symmetry reasons. The AOM energy matrix elements calculated with respect to these orbitals from the models d and f are compiled in Appendix 2. Some of these have been published earlier [18]. On this basis the general D_3 matrix elements for quartet d^3 states are obtained using the cubic strong field wave functions $|\alpha S\Gamma M_S M_\Gamma\rangle$ as a basis (cf. in Table A2 in this appendix). Due to the small spin-orbit coupling matrix elements combining with doublet states can be neglected.

Table 2. Flow diagram for possible angular overlap models

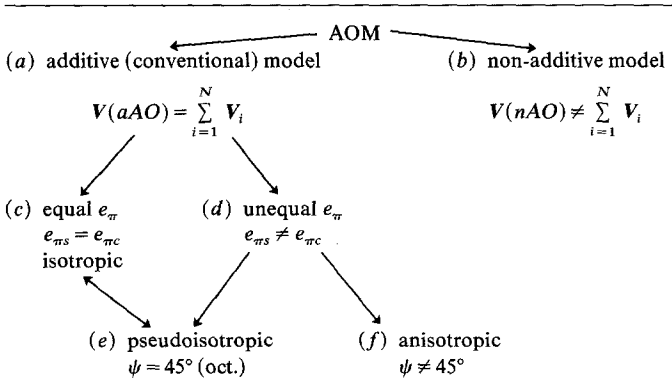

A more profound extension of the AOM which becomes important for chelate complexes is based on an idea of Orgel [5] by considering the phase relations of ligand orbitals which can influence the d-orbital splitting in a different way as the point symmetry of the chromophore would predict. Most recently this model has been introduced into the AOM [6] and the elaboration of the formalism has led to a non-additive model for the metal-ligand interactions due to the phase coupling inside the chelate ring (model b). Since we want to use a different parametrization which is more consistent to the common AOM as that in the earlier work [6] the coupling model is briefly presented in the following.

Let us consider the π-electron system of a bidentate d-electron metal $M(A-A)$ with in phase and out of phase relations between orbitals on the atoms A attached to the metal M (Fig. 2). In the additive model, considering anisotropic π-bonding (model d), the AOM energy matrix for the d_{xz}, d_{yz}, d_{xy} orbitals is diagonal

$$V(aAO)=\begin{pmatrix} e_{\pi s} & 0 & 0 \\ 0 & e_{\pi s} & 0 \\ 0 & 0 & 2e_{\pi c} \end{pmatrix} \tag{3}$$

and neglects the phase relations of ligand orbitals. Introducing orbital symmetries in model b, the basis set is classified by irreducible representations of point symmetry C_{2v} leading to symmetry orbitals

$$\begin{aligned} b_1 \quad & d\psi=\sqrt{1/2}(d_{xz}+d_{yz}) \\ a_2 \quad & d\chi=\sqrt{1/2}(d_{xz}-d_{yz}) \\ a_1 \quad & d_{xy}. \end{aligned} \tag{4}$$

Since only z-dependent orbitals are involved due to the symmetry adaptation by transformation matrix

$$T=\sqrt{1/2}\begin{pmatrix} 1 & 1 \\ 1 & -1 \end{pmatrix} \tag{5}$$

we can limit on this subspace for which the AOM energy matrix arising from perturbation by interaction with ligand orbitals ψ and χ is

$$V_{\pi s}=\begin{pmatrix} e_{\pi s} & 0 \\ 0 & e'_{\pi s} \end{pmatrix}. \tag{6}$$

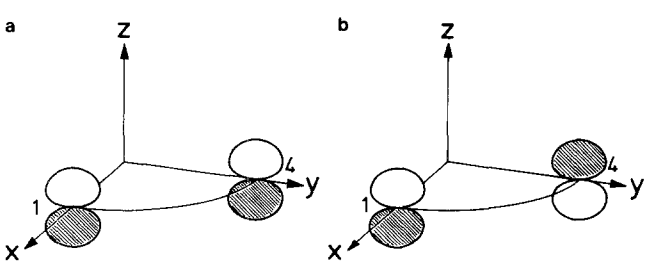

Fig. 2. π-Orbital phase coupling scheme for bidentate ligands **a** in phase ψ-type coupling b_1 in C_{2v} notation, **b** out of phase χ-type coupling a_2

Since the free ligand ψ- and χ-orbitals have in general different molecular orbital energies, the parameters $e_{\pi s}$ and $e'_{\pi s}$ are in unequal.[1] A transformation back into the d-orbital basis set leads to

$$\boldsymbol{V}_{\pi s} = \boldsymbol{T}^{-1}\boldsymbol{V}_{\pi s}\boldsymbol{T} = (1/2)\begin{pmatrix} e_{\pi s}+e'_{\pi s} & e_{\pi s}-e'_{\pi s} \\ e_{\pi s}-e'_{\pi s} & e_{\pi s}+e'_{\pi s} \end{pmatrix} \tag{7}$$

which in the case $e_{\pi s} = e'_{\pi s}$ is identical to the e_π-depending part of the aAO-matrix Eq. (3) where phase coupling is neglected. Due to the finite off-diagonal element in Eq. (7) for $e_{\pi s} \neq e'_{\pi s}$, a three-center interaction via d_{xz} and d_{yz} is introduced which destroys the additivity rule valid in LFT and in other versions of AOM.

For orthoaxial tris-chelate complexes the trigonal AOM matrix for tetragonally quantized orbitals d_{xz}, d_{yz}, d_{xy} in the nAO model b is

$$\boldsymbol{V}_{\pi}^{\text{trig}} = \begin{pmatrix} e_{\pi s}+e'_{\pi s}+2e_{\pi c} & (1/2)(e_{\pi s}-e'_{\pi s}) & (1/2)(e_{\pi s}-e'_{\pi s}) \\ & e_{\pi s}+e'_{\pi s}+2e_{\pi c} & -(1/2)(e_{\pi s}-e'_{\pi s}) \\ & & e_{\pi s}+e'_{\pi s}+2e_{\pi c} \end{pmatrix}. \tag{8}$$

Since the matrix is symmetric, off-diagonal elements V_{ij} for $i>j$ are omitted. In case of a general (not orthoaxial) orientation of the main MA_6 axes the corresponding matrix can be easily constructed using the familiar angular parts $F_\lambda(\theta, \phi)$ of the AOM which only depend on the geometry of the molecule [19]. Neglecting phase coupling and π-anisotropy, i.e. $e_{\pi s} = e'_{\pi s} = e_{\pi c}$, Eq. (8) simplifies to a matrix having only $4e_\pi$ elements on the diagonal which corresponds to an octahedral perturbation energy in the conventional AOM model a. The σ part arising from the d_{z^2} and $d_{x^2-y^2}$ remains unchanged; the perturbation matrix due to σ-interaction with corresponding orbitals of the ligands is taken from the additive model a and has for an octahedral arrangement of ligands $3e_\sigma$ on the diagonal with vanishing off-diagonal elements. The quartet state d^3 matrix elements for ligands located on the coordinate axes x, y, z for a non-additive trigonal ligand field are listed in Table A2 of Appendix 2.

3. Results and discussion

In Fig. 3 quartet absorption spectra of the title compounds doped in their aluminium hosts recorded by using different polarizations with respect to the optical axes are presented. They agree with the spectra of Piper and Carlin [8, 10], the polarizations of the acetylacetonate spectrum being in variance with those reported by Chakravorty and Basu [20]. Our spectra in addition exhibit more details for the higher energy bands. The assignments obtained from D_3 selection rules for polarized transitions are given in Table 3. Since the α-spectrum coincides with the σ-spectrum and is different from the π-spectrum, the intensity is primarily due to an electric dipole mechanism. Only one trigonal split component of the second quartet band ($^4A_{2g} \rightarrow {}^4T_{1g}$ in O_h notation) is dipole allowed and is observed

[1] Notice that in the earlier work [6] both the parameters have been set equal to $2e_{\pi\perp}$ using a baricenter rule which actually is not applicable in this instance

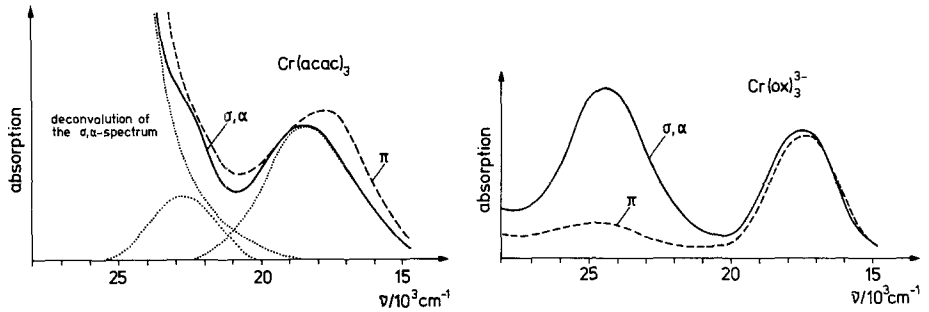

Fig. 3. Polarized absorption spectra of $Cr(acac)_3$ and $Cr(ox)_3^{3-}$ doped in corresponding aluminium host lattices at liquid nitrogen temperature

as σ-polarized transition $^4A_2 \rightarrow {}^4E$ in D_3 notation. In the case of $Cr(acac)_3$ the corresponding band, which is partially covered by strong charge-transfer absorption [8], is derived from band deconvolution. Assignment to a *d-d* transition then is strongly supported by its spectral position, lineshape, and extinction coefficient. The symmetry forbidden $^4A_2 \rightarrow {}^4A_2$ transition that is detected as a weak band only in the π-spectrum of $Cr(ox)_3^{3-}$ probably obtains its intensity by an elaborate vibronic coupling mechanism which is of no interest here.

As already indicated in the introduction the trigonal splitting of the first O_h band is large for the acac compound, even larger than for the ox complex, although its geometric structure is closer to octahedral than for the ox compound, the latter showing definite nuclear distortions to trigonal symmetry. In the following we want to explain these findings which are beyond expectations by applying different versions of the AOM outlined in the theoretical part. The calculations are limited by considering the geometric factors obtained from X-ray structure investigations for the pure complexes and their host lattice compounds (Table 1) since no large changes are expected for the doped systems. So, any calculation performed for reproducing the electronic level system of the present compounds which starts from the ground state should vary the experimental geometric factors only to a relatively small amount. For acetylacetonate compounds, which have planar ligands in the complex also, restrictions due to the angular relations Eq. (1) and (2) must be obeyed.

On Fig. 4 the variation of quartet state levels with structural angles θ, ϕ and ψ, respectively, in the additive model *a* is presented keeping the other angles constant at their octahedral value. The AOM parameter set e_σ, e_π and B (Racah-parameter) is chosen on the basis of ligand field results obtained from the doped $Cr(acac)_3$ system (12). Figure 4a and b refers to the isotropic model *c* or in the particular case $\psi = 45°$ to the pseudoisotropic model *d* if $e_{\pi s}$ is chosen different from $e_{\pi c}$. Moreover, for nonplanar ligands as in oxalate complexes the structural angles may vary independently. The plots then can be used as a guide for assigning the band features in the absorption spectra which exhibit characteristic ligand field splittings due to trigonal symmetry within the model *a*.

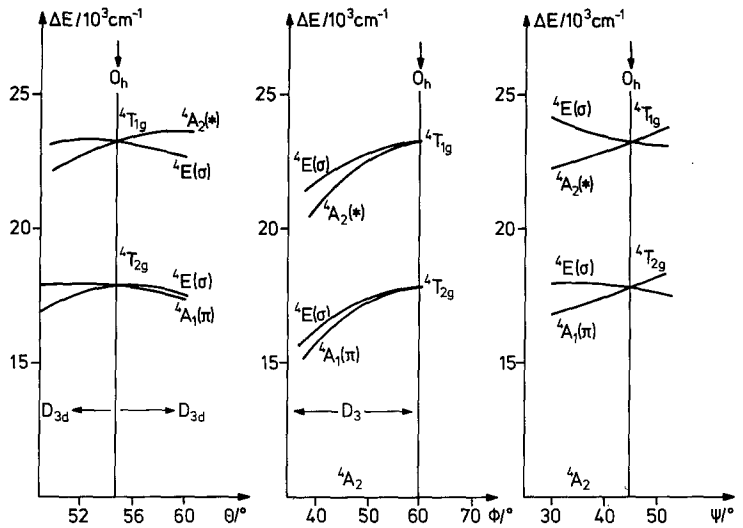

Fig. 4. Quartet level diagrams calculated from different additive AOMs (see text) with varying structural angles. The model parameters (in cm^{-1}) used are $e_\sigma = 7300$, $e_{\pi s} = 2000$, $e_{\pi c} = 0$, $B = 500$ for **a** $\phi = 60°$, $\psi = 45°$; **b** $\theta = 54.74°$, $\psi = 45°$; **c** $\theta = 54.74°$, $\phi = 60°$

Evidently the calculated splittings are most sensitive particularly to small variations of the polar angle θ (Fig. 4a). For a geometry very close to octahedral which is realized in the $Cr(acac)_3$ complex one obtains the experimental sequence $A_1 < E$ (from T_{2g}) for a compressed octahedron, i.e. $\theta > 54.74°$, with ϕ and ψ angles smaller than its octahedral values (cf. Table 3). Using the actual X-ray data in the calculation the reverse order $E < A_1$ is obtained. In either case the level splitting is calculated one order of magnitude lower ($\sim 80\ cm^{-1}$) than experimentally found ($800\ cm^{-1}$). Correct level relations and larger splittings are only obtained if a geometric structure of the chromophore in the host is taken

Table 3. Experimental[a] and calculated quartet energy levels (best fit) of $Cr(acac)_3$ and $Cr(ox)_3^{3-}$ (in cm^{-1})

$Cr(acac)_3$		Assignment			$Cr(ox)_3^{3-}$	
experimental	calculated[b]	D_3	O_h	D_3	experimental	calculated[c]
17 700(π)[d]	17 700	A_1	T_{2g}	A_1	17 300(π)	17 250
18 500(σ)	18 500	E		E	17 500(σ)	17 500
	22 100	A_2	T_{1g}	E	24 300(σ)	24 400
22 700(σ)[f]	23 400	E		A_2	24 600(*)	24 650

[a] Doped in isomorphous Al-compounds
[b] Best fit parameters $3e_\sigma - 2e_{\pi s} - 2e_{\pi c} = 18\,400$, $e_{\pi s} = 1400$, $B = 400$
[c] Best fit parameters $e_\sigma = 6750$, $e_{\pi s} = e_{\pi c} = 530$, $B = 710$, $\theta = 56.3°$
[d] Observed polarizations are given in parenthesis; *-forbidden transition
[e] Not observed
[f] Broad shoulder, peak maximum is obtained from a band deconvolution

which is far away (e.g. $\theta = 58°$ and $\phi = 45°$) from the X-ray data obtained for the pure compounds and the Al lattice. The extension to the anisotropic model *f* using different parameters $e_{\pi s}$, $e_{\pi c}$ and varying ψ slightly from its octahedral number $\psi = 45°$ does not change the situation essentially since with ψ values around 45° we are close to the pseudoisotropic model *e* which yields similar results to those obtained from the isotropic model *c*. The spectrum of $Cr(acac)_3$, therefore, cannot be understood within the additive model *a* if the calculations start from a geometric structure in the ground state which is close to an octahedron and preserving the planarity of the chelate ligand.

The large band splittings also cannot be calculated from a Jahn-Teller effect in the excited states. These are for octahedral Cr(III) complexes $^4T_{2g}$ and $^4T_{1g}$ and could be, in principle, split by vibronic coupling to Jahn-Teller active τ_{2g} modes leading to the observed trigonal splitting of these levels. A short look on the vibronic energy matrix for $T_2 \times \tau_2$ coupling shows, however, that this Jahn-Teller coupling is also not able to explain the $Cr(acac)_3$ spectrum. The eigenvalues of the first order Jahn-Teller coupling matrix are

$$e_1 = 2FQ_0 \quad \text{and} \quad e_2 = e_3 = -FQ_0 \tag{9}$$

where $F = (T_2\eta|(\partial V/\partial Q_\xi)_0|T_2\zeta)$ is a matrix element of different components η, ζ of T_2 eigenfunctions and Q_0 is the minimal coordinate $Q_0 = -(2/3)F/K$ with K denoting the quadratic force constant of τ_2 vibration [21]. Introducing into F one-electron functions leads to $F = (1/2)(\eta|(\partial V/\partial Q_\xi)_0|\zeta)$ that combines only π-functions out of the *xy*, *xz* and *yz* *d*-orbital set which is known to cause only small Jahn-Teller forces due to weak anti-bonding. The calculation of the integral F by the additive AOM model *d* following the method of Bacci [22] yields

$$F = (1/2)(e_{\pi c} + e_{\pi s})/R \tag{10}$$

allowing an estimate for the $^4T_{2g}$ splitting due to the τ_2 Jahn-Teller coupling of 50 to 200 cm^{-1}. This is much smaller compared to the 800 cm^{-1} found experimentally (Table 3). We conclude that common AOM is not able to explain the measured spectra properly. The discussion must therefore consider a more general model (vide infra). We turn, however, at first to the oxalate spectrum.

For the oxalate chromium(III) complex doped into $A_2B(Al(ox)_3)\cdot nH_2O$ host lattices with various cations K, Na, NH_4 or $A_2 = Mg$ always a level ordering of $A_1 < E < E < A_2$ as given in Table 3 is obtained in all instances although the actual level energies vary unusually large [23]. The plots on Fig. 4 reproduce the band splittings due to transitions into the first spin-allowed octahedral $^4T_{2g}$ state quite well for any of the variations close to the geometry angles obtained from the X-ray structure investigation of $K_3Cr(ox)_3$ as listed in Table 1. The higher levels, on the other hand, are only calculated leading to the correct order and level splittings large enough in energy, if the polar angle is $\theta > 56°$ which would exceed the corresponding structural angles obtained for the pure compounds by a very small amount. This holds for the isotropic model *c* depicted as solid line in Fig. 5; a calculation with the same parameters $\phi = 48°$, $e_\sigma = 7000$ cm^{-1} and $B = 700$ cm^{-1} applying the anisotropic model *f* with $\psi = 40°$ marked as dashed lines

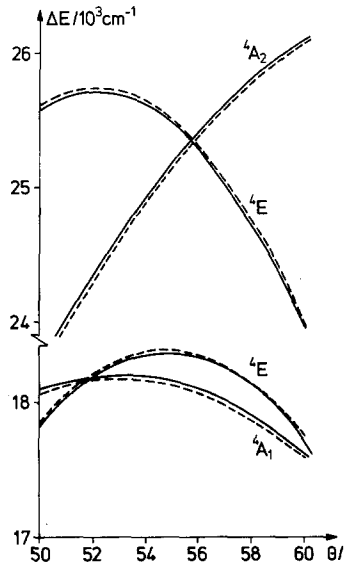

Fig. 5. Quartet level diagram for structural angles adapted to $Cr(ox)_3^{3-}$ geometry with parameters (in cm^{-1}) $e_\sigma = 7000$, $B = 700$ calculated by the model c using $e_\pi = 500$ and $\phi = 48°$, $\psi = 45°$ (*solid lines*) and by model f using $e_{\pi s} = 600$, $e_{\pi c} = 400$ and $\phi = 48°$, $\psi = 40°$ (*dashed lines*)

in that figure changes the levels only slightly, therefore an extension of the model is felt not to be necessary. We conclude that the additive isotropic model c, i.e. the conventional AOM, is able to account for the proper quartet splittings of Cr(III) tris-oxalate complexes. The significant deviation from planarity described by the angle γ in Table 1 allows for choosing the ψ angle independently from θ and ϕ which can serve for a better optimization on reproducing the experimental data. We do not want to go into further details. The AOM parameters of $Cr(ox)_3^{3-}$ (cf. Table 3) obtained from a best fit to the spectrum are similar to those reported from corresponding carboxylate complexes [3]. Concerning the larger polar angle $\theta > 56°$ derived from the spectrum of the doped materials ($\theta = 56.3°$ for $K_3Cr(ox)_3$) indicating a compression along the trigonal axis of the guest molecule in the host lattice, it should be pointed out that this is to be expected in view of the larger metal-oxygen distances for the Cr compound compared to the Al host (see the R values given in Table 1).

Finally we come to the problem of explaining the spectrum of $Cr(acac)_3$ by the use of the non-additive model b; in particular the question should be answered why this model must be applied in this case and not to other chelates as to $Cr(ox)_3^{3-}$. Since acetylacetonate and oxalate ligands are oxygen donors ($e_\pi > 0$) it is the highest occupied orbitals (HOMO's) which interact with the d-orbitals of the metals. A routine ab initio calculation, performed with a Gaussian 82 program [24] with STO-3G and 4-31G basis sets implemented therein using experimental geometric parameters for the free acac ligand gave a ψ-type function for the highest occupied π-orbital π_3, i.e. an in phase coupling of terminal atomic orbitals (Fig. 2); the lower π-orbital π_2 is of χ-type, out of phase, it is more than 4 eV below the π_3 orbital indicating that its interaction with d-orbitals should be rather small so that the corresponding $e'_{\pi s}$ parameter in the AOM matrix

Eq. (8) can be neglected. In this case the d^3 matrix elements for an octahedral arrangement of the oxygen atoms listed in Table A2 of the Appendix 2 are applicable. The corresponding level scheme calculated from an appropriate set of AOM parameters (vide infra) is presented in Fig. 6. The results show that not only the level order for the first spin-allowed transitions is correctly reproduced but also the large low symmetry splitting of about 800 cm^{-1} for the $^4T_{2g}$ level is obtained although the calculations start from a perfect octahedral ground state geometry of the CrO_6 chromophore. The actual parameter values could not be determined since one of the band components arising from the second spin allowed $^4T_{1g}$ level is not detected in the spectrum since its transition is forbidden according to symmetry selection rules. They can, however be estimated from approximate relations obtained by using overlap considerations [25] and diagonal element expressions from the perturbation matrix of Table A2 which are fitted to the experiment:

$$\begin{aligned} &e_{\pi c}/e_{\pi s} = 0.60 \\ &3e_\sigma - e_{\pi s} - 2e_{\pi c} = 18\,600\ \text{cm}^{-1}. \end{aligned} \tag{11}$$

Together with the $e_{\pi s}$ parameters obtained from the observed trigonal splitting of the first transition the AOM parameters for $Cr(acac)_3$ are estimated as e_σ = 7400–7700 cm^{-1}, $e_{\pi s}$ = 1400–2000 cm^{-1} and $e_{\pi c}$ = 800–1200 cm^{-1} which is a reasonable result comparing to what is reported for other acetylacetonate complexes [3, 26, 27]. Although the t_{2g}-orbital energies are split due to the complex D_3 symmetry by an appreciable amount, the molecule remains octahedral since due to the large spin-pairing energy the three d-electrons are equally distributed over the three orbitals forming a quartet state and balancing out any possible gain in energy due to larger distortions. The corresponding $Co(acac)_3$ complex has lower symmetry [28] with larger bite angles of the chelate ligands because of the smaller ionic radius of Co(III) compared to Cr(III).

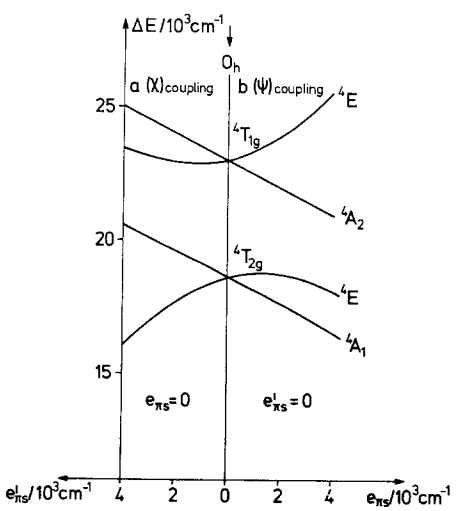

Fig. 6. Quartet level plot calculated by the non-additive model *b* for a complex with ligand donor atoms being octahedrally located ($\theta = 54.74°$, $\phi = 60°$, $\psi = 45°$) for either ψ-type or χ-type coupling using model parameters $3e_\sigma - e_{\pi s} - 2e_{\pi c} = 18\,600$ (see text) and $B = 400\ cm^{-1}$

For the oxalate ligand the highest occupied π-orbitals are also of ψ- and χ-symmetry type, their energies are, however, calculated, using the same *ab initio* program and identical orbital basis sets as for the acetylacetonate ligand, to be almost equal. For degenerate ligand orbitals interacting with metal d-orbitals, the AOM parameters become identical, i.e. $e_{\pi s} = e'_{\pi s}$. This carries the perturbation matrix Eq. (8) over into a matrix with only elements $2(e_{\pi s} + e_{\pi c})$ on the diagonal which corresponds to an octahedral AOM perturbation matrix in the additive model *a*. Therefore, we can conclude, that for degenerate π-orbitals which interact with the d-function of the central metal by the same amount yielding equal perturbation energies, the non-additive model *b* does not apply, the perturbation expressions transform into the more simple case of the additive model *a* with isotropic *c* or anisotropic *f* π-bonding behaviour. The same arguments can be brought forward, when instead of Eq. (8) the correct perturbation matrix is used which considers the actual (non-octahedral) valence angles of $Cr(ox)_3^{3-}$. The AOM parameters adapted from a best fit to the experimental level energies for $Cr(ox)_3^{3-}$ (Table 3) are $e_\sigma = 6750\ cm^{-1}$, $e_\pi = 530\ cm^{-1}$ and $B = 710\ cm^{-1}$. They are consistent with the corresponding $Cr(acac)_3$ parameters indicating an increased covalent bonding in the acetylacetonate complex which is reflected from the larger AOM parameters e_σ, e_π and the more pronounced nephelauxetic effect as well, i.e. the smaller Racah-parameter $B = 400\ cm^{-1}$ for $Cr(acac)_3$ compared to $710\ cm^{-1}$ for $Cr(ox)_3^{3-}$.

4. Conclusions

The present application of the AOM shows that this model is flexible enough for introducing a variety of extensions which are necessary for rationalizing the energy level schemes derived from absorption spectra of chelate complexes. Using a non-additive model band splittings are calculated, in particular for compounds exhibiting no distortions of nuclear ground state geometry, which cannot be obtained by the impact of Jahn-Teller effects.

Appendix 1

For deriving Eq. (1) the normals $\bar{n} = \overline{MA_4} \times \overline{MA_1}$ and $\bar{n}' = \overline{Mz'} + \overline{MA_4}$ on the planes A_1MA_4 and $z'MA_4$, respectively, are considered (cf. Fig. 1). The angle ψ at ligand 4 is

$$\cos\psi = \bar{n} \cdot \bar{n}' / (|\bar{n}| \cdot |\bar{n}'|) \tag{A1}$$

since $\bar{n}$ and $\bar{n}'$ have the components ($R = 1$)

$\bar{n}$:	$-\cos\theta \sin\theta \sin\phi$	$\sin\theta \cos\theta(1+\cos\phi)$	$-\sin^2\theta \sin\phi$
$\bar{n}'$:	$-\sin\theta \sin\phi$	$\sin\theta \cos\phi$	0

and the lengths $|\bar{n}| = \sin \alpha$ (bite angle) and $|\bar{n}'| = \sin \theta$. Substitution into (A1) yields

$$\cos \psi = \cos \theta \cdot \cos (\phi/2)/\sin (\alpha/2) \tag{A2}$$

which is Eq. (1) in the text. Equation (2) is obtained by forming the scalar product of the bond vectors $\overline{MA_4}$ and $\overline{MA_1}$.

Appendix 2

The non-vanishing trigonal (D_3) AOM matrix elements within the additive model *a* for anisotropic π-bonding, model *f*, for a *d*-orbital set in trigonal quantization (coordinate system as in Fig. 1) are given in Table A1. The notations are explained in the text. For the case of a d^3 electron configuration the strong field wave functions adapted to cubic symmetry given by Tanabe and Sugano [29] have been used. The quartet functions are numbered by standard order t_2^3: $^4A_2(1)$, t_2^2e: $^4T_1\alpha(2)$, $^4T_1\beta(3)$, $^4T_1\gamma(4)$, $^4T_2\xi(5)$, $^4T_2\eta(6)$, $^4T_2\zeta(7)$, t_2e^2: $^4T_1\alpha(8)$, $^4T_1\beta(9)$, $^4T_1\gamma(10)$. In Table A2 the non-vanishing matrix elements for the anisotropic model *f* in terms of the one-electron matrix elements of Table A1 are listed (left column). Also the d^3 matrix elements of the non-additive model *b* for a ψ- and χ-type perturbation are given in the case of octahedrally coordinated ligator atoms which are located on the cartesian coordinate axes *x*, *y*, *z* (tetragonally quantized *d*-orbital set).

Table A1. Trigonal AOM D_3-matrix elements for symmetry adapted *d*-orbitals

$$a = (z^2|V(D_3)|z^2) = (3/8)(1+3\cos 2\theta)^2 e_\sigma + (9/2)\sin^2 2\theta \sin^2 \psi e_{\pi s} + (9/2)\sin^2 2\theta \cos^2 \psi e_{\pi c}$$

$$b = (xz|V(D_3)|xz) = (yz|V(D_3)|yz)$$
$$= (9/4)\sin^2 2\theta e_\sigma + 3(\cos^2 \theta \cos^2 \psi + \cos^2 2\theta \sin^2 \psi) e_{\pi s} + 3[\cos^2 \theta \sin^2 \psi + \cos^2 2\theta \cos^2 \psi] e_{\pi c}$$

$$c = (xy|V(D_3)|xy) = (x^2-y^2|V(D_3)|x^2-y^2)$$
$$= (9/16)(1-\cos 2\theta)^2 e_\sigma + 3[\sin^2 \theta \cos^2 \psi + (1/4)\sin^2 2\theta \sin^2 \psi] e_{\pi s}$$
$$+ 3[\sin^2 \theta \sin^2 \psi + (1/4)\sin^2 2\theta \cos^2 \psi] e_{\pi c}$$

$$d = (xz|V(D_3)|x^2-y^2) = -(yz|V(D_3)|xy)$$
$$= (9/16)\sin 2\theta(1-\cos 2\theta)(1-\cos 3\phi) e_\sigma + (3/4)\sin 2\theta(-1+\cos 3\phi)[\cos^2 \psi e_{\pi s} + \sin^2 \psi e_{\pi c}]$$
$$+ (3/8)\sin 4\theta(1-\cos 3\phi)[\sin^2 \psi e_{\pi s} + \cos^2 \psi e_{\pi c}]$$
$$+ (3/8)\sin 2\psi \sin 3\phi[\cos \theta \sin 2\theta + 2\sin \theta \cos 2\theta](-e_{\pi s} + e_{\pi c})$$

$$f = (yz|V(D_3)|x^2-y^2) = (xz|V(D_3)|xy)$$
$$= -(9/16)\sin 2\theta(1-\cos 2\theta)\sin 3\phi e_\sigma + (3/8)\sin 3\phi[2\sin 2\theta \cos^2 \psi - \sin 4\theta \sin^2 \psi] e_{\pi s}$$
$$+ (3/8)\sin 3\phi[2\sin 2\theta \sin^2 \psi - \sin 4\theta \cos^2 \psi] e_{\pi c}$$
$$+ (3/8)\sin 2\psi(1-\cos 3\phi)[\cos \theta \sin 2\theta + 2\sin \theta \cos 2\theta](-e_{\pi s} + e_{\pi c})$$

Table A2. Quartet state matrix elements of the trigonal ligand field for a d^3 configuration

Matrix element	Additive field	Non-additive field[a]
(1|1)	$2b+c-15B$	$-15B$
(1|2)	$-(\sqrt{3}/2)f$	0
(2|2)	$b+(7/4)c+(1/4)a-3B$	$3e_\sigma-e_{\pi s}-e'_{\pi s}-2e_{\pi c}-3B$
(1|3)	$(\sqrt{3}/2)d$	0
(2|3)	0	$(1/4)(e_{\pi s}-e'_{\pi s})$
(3|3)	$b+(7/4)c+(1/4)a-3B$	$3e_\sigma-e_{\pi s}-e'_{\pi s}-2e_{\pi c}-3B$
(2|4)	$-d/2$	$-(1/4)(e_{\pi s}-e'_{\pi s})$
(3|4)	$f/2$	$(1/4)(e_{\pi s}-e'_{\pi s})$
(4|4)	$2b+a-3B$	$3e_\sigma-e_{\pi s}-e'_{\pi s}-2e_{\pi c}-3B$
(1|5)	$-f/2$	0
(2|5)	$(\sqrt{3}/4)(c-a)$	0
(3|5)	0	$(\sqrt{3}/4)(e_{\pi s}-e'_{\pi s})$
(4|5)	$(\sqrt{3}/2)d$	$(\sqrt{3}/4)(e_{\pi s}-e'_{\pi s})$
(5|5)	$b+(5/4)c+(3/4)a-15B$	$3e_\sigma-e_{\pi s}-e'_{\pi s}-2e_{\pi c}-15B$
(1|6)	$-d/2$	0
(2|6)	0	$-(\sqrt{3}/4)(e_{\pi s}-e'_{\pi s})$
(3|6)	$(\sqrt{3}/4)(a-c)$	0
(4|6)	$(\sqrt{3}/2)f$	$(\sqrt{3}/4)(e_{\pi s}-e'_{\pi s})$
(5|6)	0	$(1/4)(e_{\pi s}-e'_{\pi s})$
(6|6)	$b+(5/4)c+(3/4)a-15B$	$3e_\sigma-e_{\pi s}-e'_{\pi s}-2e_{\pi c}-15B$
(2|7)	$-(\sqrt{3}/2)d$	$-(\sqrt{3}/4)(e_{\pi s}-e'_{\pi s})$
(3|7)	$-(\sqrt{3}/2)f$	$-(\sqrt{3}/4)(e_{\pi s}-e'_{\pi s})$
(5|7)	$-d/2$	$-(1/4)(e_{\pi s}-e'_{\pi s})$
(6|7)	$f/2$	$(1/4)(e_{\pi s}-e'_{\pi s})$
(7|7)	$2b+c-15B$	$3e_\sigma-e_{\pi s}-e'_{\pi s}-2e_{\pi c}-15B$
(2|8)	$6B$	$6B$
(4|8)	d	0
(8|8)	$a+b+c-12B$	$6e_\sigma-2e_{\pi s}-2e'_{\pi s}-4e_{\pi c}-12B$
(3|9)	$6B$	$6B$
(4|9)	$-f$	0
(8|9)	0	$(1/2)(e_{\pi s}-e'_{\pi s})$
(9|9)	$a+b+c-12B$	$6e_\sigma-2e_{\pi s}-2e'_{\pi s}-4e_{\pi c}-12B$
(2|10)	$d/2$	0
(3|10)	$-f/2$	0
(4|10)	$6B$	$6B$
(5|10)	$-(\sqrt{3}/2)d$	0
(6|10)	$-(\sqrt{3}/2)f$	0
(8|10)	$-d$	$-(1/2)(e_{\pi s}-e'_{\pi s})$
(9|10)	f	$(1/2)(e_{\pi s}-e'_{\pi s})$
(10|10)	$a+2c-12B$	$6e_\sigma-2e_{\pi s}-2e'_{\pi s}-4e_{\pi c}-12B$

[a] The non-additive ligand field matrix elements apply for ligands located on the cartesian axes x, y and z

References

1. Jørgensen CK, Pappalardo R, Schmidtke H-H (1963) J Chem Phys 39:1422
2. Jørgensen CK (1971) Modern aspects of ligand field theory. North Holland, Amsterdam
3. Smith DW (1978) Struct and Bonding 35:87
4. Burdett JK (1980) Molecular shapes. Wiley, New York
5. Orgel LE (1961) J Chem Soc 3683
6. Ceulemans A, Dendooven M, Vanquickenborne LG (1985) Inorg Chem 24:1153
7. Glerup J, Monsted O, Schäffer CE (1976) Inorg Chem 15:1399
8. Piper TS, Carlin RL (1962) J Chem Phys 36:3330
9. Morosin B (1965) Acta Cryst 19:131
10. Piper TS, Carlin RL (1961) J Chem Phys 35:1809
11. Taylor D (1978) Aust J Chem 31:1455
12. Schönherr T, Eyring G, Linder R (1983) Z Naturforschung 38a:736
13. Schoenen N, Schmidtke H-H (1986) Mol Phys 57:983
14. Urushiyama A, Schönherr T, Schmidtke H-H (1986) Ber Bunsenges Phys Chem 90:1195
15. Larsen E, La Mar GN (1974) J Chem Educ 51:633
16. Hon PK, Pfluger CE (1973) J Coord Chem 3:67
17. Schäffer CE (1968) Struct and Bonding 5:68
18. Nikolov GS, Trendafilova NS (1979) Soviet J Coord Chem 5:254
19. Schäffer CE, Jørgensen CK (1965) Mol Phys 9:401
20. Chakravorty A, Basu S (1961) J Chem Phys 33:1266
21. Bersuker IB (1984) The Jahn-Teller effect and vibronic interactions in modern chemistry. Plenum Press, New York
22. Bacci M (1979) Chem Phys 40:237
23. Spanier J (1985) Diplomarbeit, University Düsseldorf
24. Pople JA et al. (1982) Program Gaussian 82, Carnegie-Mellon-University, Pittsburgh, PA
25. Atanasov MA, Nikolov GS (1983) Comm Dep Chem Bulg Acad Sci 16:329
26. Hitchman MA (1972) J Chem Soc Faraday Trans 68:846
27. Atanasov MA, Nikolov GS (1983) Inorg Chim Acta 72:95
28. Moucharafieh NC, Eller PG, Bertrand JA, Royer DJ (1978) Inorg Chem 17:1220
29. Sugano S, Tanabe Y, Kamimura H (1970) Multiplets of transition metal ions in crystals. Academic Press, New York